

Comparison of NDVI of ground measurement, atmospheric corrected ASTER L1B data and ASTER surface reflectance product (AST07) data

Buhe Aosier and Masami Kaneko

Department of Biosphere and Environmental Sciences,
Rakuno Gakuen University,
Bunkyo-dai-Midorimachi, 582, Ebetsu, 069-8501, Japan
e-mail: aosier@rakuno.ac.jp

Masayuki Takada

Hokkaido Institute of Environmental Sciences,
Kitaku-Kita 19, Nishi-12, Sapporo, 060-0912, Japan.
e-mail: mtakada@hokkaido-ies.go.jp

Abstract— In this study, we comparison of NDVI of ground measurement, atmospheric corrected ASTER L1B data and ASTER surface reflectance product (AST07) data to evaluate the accuracy of the ATCOR software atmospheric correction of Terra/ASTER data (Jun 30, 2002), using ground radiometric measurement data (ASD's FieldSpec® Pro). Our research selected the study area Sarobetsu Marsh located in coastal area of Hokkaido, Japan. We found that 5% of scattering radiation is contained with the ASTER Green band and 47% of radiation was absorbed in the ASTER NIR band and 17% of radiation was absorbed in the ASTER SWIR6 band. And that the ASD's measurement values and the ATCOR software output values are no big difference in the ASTER reflection band and absorption bands of chlorophyll (i.e. NIR-band and Red-band); However, the difference was see in the ASTER scattering bands (i.e. visible Green band) and soil reflection bands (i.e. ASTER SWIR bands). Compared with the data of ASD's measurement, the AST07 (©NASA/EOSDIS ASTER surface reflectance product data (L2B)) values are too low in a NIR band.

Keywords: NDVI, ASTER L1B & AST07, ASD's FieldSpec®, surface reflectance, ground measurement.

1. INTRODUCTION

Radiation from the Earth's surface undergoes significant interaction with the atmosphere before it reaches the satellite sensor. Regardless of the type of analysis that is performed on the remotely sensed data, it is important to understand the effect the atmosphere has made to the radiance responses [1]. In order to acquire an exact radiation of target, we must correct the atmosphere effect of satellite imagery. Correction of image data for the effects of atmospheric propagation can be carried out in essentially three ways [2]. It is respectively, based on atmospheric scattering and absorption characteristics physically model; Based on pre-calibration, on-board calibration against targets of known reflectance method and Based on dark-pixel

subtraction method. The physically based methods attempt to model are (for example, Look-up table (LUT) approach and top-of atmosphere (TOA) radiance) is the most rigorous approach, and also the most difficult to apply [3]. The atmospheric scattering and absorption characteristics area calculated by a computer model (the best-known being LOWTRAN-7 [4], MODTRAN [5] [6] and 6S [7] which requires as input data meteorological, seasonal and geographical variables. In practice, these variables may not all be available with sufficient spatial or temporal resolution, and, in particular, estimation of the contribution of atmospheric aerosols is difficult [3] [8]. In the calibration based atmospheric correction of VNIR, SWIR imagery method, these targets can be artificially constructed or naturally occurring, but they need to satisfy a number of criteria: (1) their reflectances must be known sufficiently accurately, in the same spectral bands as are used by the imager; (2) the range of reflectances represented by the calibrators must span the range of interest in the sensor; (3) each calibrator should cover an area of at least several rezeles; (4) the calibrators should be well distribution over the entire scene, so that possible variation of atmospheric conditions from place to place can be assessed and if necessary, allowed for [3] [9]. Dark pixel subtraction is a technique which determines the pixel in the image with the lowest brightness value. This pixel is assumed to have a zero ground reflectance such that its radiometric value represents the additive effect of the atmosphere [10]. This method is quite crude: it assumes that the minimum reflectance in each band is zero, that the atmospheric correction can be modeled adequately as an additive effect, and that the correction does not vary from place to place within the scene. To some extent, visual inspection of an image can determine whether these assumptions are likely to be valid. Zero-reflectance rezeles can be provided by shadows and, in the near-infrared region, by water bodies [3] [11] [12].

In this study, we evaluate the accuracy of the atmosphere correction with ATCOR software algorithm based on ground radiometric measurement data, and compared also with the radiative transfer code (RTC) based atmospheric corrected ASTER L2B standard products surface reflectance (AST07) data simultaneously.

A. ATCOR software atmospheric correction method

The ATCOR software can be correct the path radiance, adjacency radiation and terrain radiation reflected to the pixel in order to calculate the reflected radiation from the viewed pixel. ATCOR2 software atmospheric correction algorithm is for a flat terrain working with an atmospheric database, and ATCOR3 software can be correct terrain radiation reflected to the pixel (from opposite hills, according to the terrain view factor) [9]. The database contains the atmospheric correction functions stored in LUT. ATCOR does the atmospheric correction by inverting the results obtained from MODTRAN, which are stored in a Look up Table. If anything, the ATCOR software method is kind of applied to the above-mentioned method of 1-the physically based methods attempt to model [13].

B. The ASTER surface reflectance product (AST07) algorithm

This Validated version of the VNIR/SWIR surface leaving radiance and reflectance products (product name: (c)NASA/EOSDIS) AST07) provide an estimate of the total radiance leaving the surface including both the reflected solar and sky components for ASTER bands 1-9. The atmospheric correction for the VNIR and SWIR is based upon LUT approach using results from a Gauss-Seidel iteration radiative transfer code [14]. The method has its basis in the reflectance-based, vicarious-calibration approach of the Remote Sensing Group at the University of Arizona [15]. We are applying the knowledge learned from our calibration methods to the atmospheric correction of the VNIR and SWIR bands for ASTER. Specifically, the RTC we have used for the past 10 years is used as a basis for LUT approach to atmospheric correction. The method currently assumes atmospheric scattering optical depths and aerosol parameters are known from outside sources. Using these parameters, a set of piecewise-linear fits are determined from the LUT that relate the measured satellite radiances to surface radiance and surface reflectance(Buhe).

II. THE DARA ANALYZED IN THIS STUDY

A. Resampling the original ASTER data

The Advanced Spaceborne Thermal Emission and Reflection Radiometer (ASTER) onboard NASA's satellite Terra is a high resolution multispectral radiometer with 14 bands, covers the visible and near-infrared (VNIR), short wave infrared (SWIR) and thermal infrared (TIR), and is effective in studying the Earth's surface land cover, vegetation and mineral resources, etc. Data used Terra/ASTER original Level 1B VNIR / SWIR/TIR Data (Time of day (UTC): 1:30, June 30, 2003, Path-108/Row-835, and 1:30, July 12, 2004, Path-109/Row-837, the subset coordinate of the UL Geo N45° 08', E141° 36') and supplied by the Earth Remote Sensing Data Analysis Center, Tokyo, Japan (©ERSDAC). In the ATCOR software, if a 14-bands ASTER image is loaded the default Layer-Band assignment will be set that input layer 13 (thermal band 13) is set to layer 10 and the output image will be restricted to 10 bands. The reason for this is that from the 5 ASTER thermal bands only band 13 is used in ATCOR. In

order to carry out calculation between bands, we re-sampling (layer stacking) this 3 layers different spatial resolution ASTER VNIR (15 m), SWIR (30 m) and TIR (90 m) data to one layer same spatial resolution (15 m) dataset, and used this dataset input to ATCOR software.

Table 1. The calibration of ASTER original LIB data (Unit: mW/cm² sr micron)

Band No.	c_0	c_1
1	-0.1	0.0676
2	-0.1	0.0708
3	-0.1	0.0862
4	-0.1	0.02174
5	-0.1	0.00696
6	-0.1	0.00625
7	-0.1	0.00597
8	-0.1	0.00417
9	-0.1	0.00318

B. ATCOR input parameters

With the ASTER data (Path-108/Row-835) data, ATCOR input parameters include: Solar zenith (degrees): **24.8**; Solar azimuth (degrees): **147.7**; Scene Visibility (km) = **30m**; Model for solar region: fall/spring/rural; various aerosol types: **rural**; Model for thermal region: **fall**. Input satellite data: subset ASTER VNIR-SWIR-TIR, **10-bands** one layer data. The calibration of ASTER data The Level 1B data are in terms of scaled radiance. To convert from DN to radiance at the sensor, the unit conversion coefficients (defined as radiance per 1 DN) are shows in Table 1. Radiance (spectral radiance) is expressed in units of **W/(m²*sr*um)**. The true radiance at sensor can be obtained from the DN values as follows:

$$L = c_0 + c_1 \times DN \quad (1)$$

Where, L is radiance. c_0 (offset) and c_1 (gain) are conversion coefficient; DN is digital number.

III. THE STUDY AREA

The study area Sarobetsu Marsh is the largest registered wetland with an area of 7000 ha located in coastal of northwestern Hokkaido, Japan (Figure 1) and nominated by the Ramsar Convention on Wetlands in 2005. Test areas are mostly swamp with *Sphagnum*, *Moliniopsis japonica* while the western coastal zone area is dominated by isolated small hills covered with broad-leaf trees. The terrain of the study area is very flat and the elevation distribution between 5 m to 15 m. We selected this study area since the natural environments are well preserved by national and municipal governments and recently, follow on drying of a swamp; here often happens that a non-moor plant (bamboo grass) invades in a swamp. In the feature, we will classified this wetland into a high moor, low

moor and non moor types, clarify the invasion front of bamboo grass, prevents that a non-moor plant (bamboo grass) re-invades in a swamp.

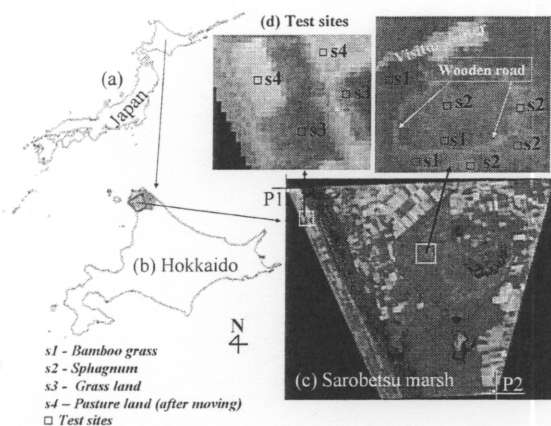


Fig. 1. Location of study area and test sites

IV. RESULT

Comparison of the ASTER data before and after ATCOR software atmospheric correction, we can summarize the following result:

(a) Shows the Table 2, the mean values of ASTER band 1 and band 2 are decrease in after atmospheric correction. This means that the visible green and red band has included not only the radiance from a target, radiance other than an atmospheric scattering also included.

(b) Comparison of mean values of NIR and SWIR bands before/after atmospheric correction, we found, the radiance values became large after atmospheric correction. It means the radiation from the target absorbed by atmosphere before it reaches the satellite sensor.

Atmospheric scattering primarily affects the direction of visible Green and Red band, and atmospheric absorption primarily affects the direction of NIR and SWIR bands.

The most significant interaction that thermal infrared radiation undergoes, as it passes through the atmosphere, is by absorption, primarily due to ozone and water vapor particles in the atmosphere. At the shorter wavelengths (i.e. Green or Red band), attenuation occurs by scattering due to clouds and other atmospheric constituents, as well as reflection. The type of scattering which the energy undergoes depends upon the size of the particle responsible. Rayleigh scattering occurs when radiation interacts with air molecules smaller than the radiation's wavelength, such as oxygen and nitrogen. The degree of scattering is inversely proportional to the fourth power of the wavelength. When particles are comparable in size to the radiation wavelength, such as aerosols, mie scattering results [16]. The effect of scattering on the visible wavelengths is significant and must be compensated for when developing empirical relationships through time [17].

Atmospheric scattering primarily affects the direction of short wave radiation. There are four types of atmospheric scattering: rayleigh, mie, raman and non selective. The most significant of these types of scattering is rayleigh scatter, which effects the short visible wavelengths and results in haze. For ASTER data the scattering is four times as great in Green band of the electromagnetic spectrum as in the NIR band.

DN of original ASTER LIB data (before correction)				
Band No.	Min	Max	Mean	Stdev
1 (Green)	0	255	50.93	34.97
2 (red)	0	210	30.83	23.15
3 (NIR)	0	179	69.82	49.02
4 (SWIR)	0	111	45.21	32.59
5 (SWIR)	0	105	27.82	20.52
6 (SWIR)	0	144	29.90	22.66
7 (SWIR)	0	155	27.49	20.41
8 (SWIR)	0	191	23.83	18.10
9 (SWIR)	0	133	21.01	15.20
DN of after ATCOR corrected ASTER data				
1 (Green)	0	229	26.47	20.16
2 (Red)	0	255	30.04	26.17
3 (NIR)	0	255	93.53	66.98
4 (SWIR)	0	224	90.89	65.64
5 (SWIR)	0	175	46.17	34.13
6 (SWIR)	0	251	51.75	39.30
7 (SWIR)	0	241	42.42	31.55
8 (SWIR)	0	255	35.86	27.33
9 (SWIR)	0	157	24.34	17.69

Shows the Figure 2(1) and 2(2), we found, the ASD's measurement values and the ATCOR output values are no big difference in the ASTER reflection bands and absorption bands of chlorophyll (i.e. NIR-band and Red-band); the difference has come out in scattering band (i.e. ASTER Green band) and soil reflection bands (i.e. ASTER SWIR bands). However, in the ©EOSDIS AST07 (ASTER surface reflectance products), the values are considerably different in ASTER NIR band. The problem is atmospheric corrected values of NIR is too small. In this research, the result of ATCOR software correction was better than AST07 products. Figure 2(1) and 2(2) shows the comparison of ATCOR software atmospheric correction result and ASTER surface reflectance products (AST07) data, with in non moor plant and high moor plant samples. In a swamp (high moor plant), the background soil and the open water area will be incorrect-recognized as moving haze of ATCOR software method. The ASTER all SWIR bands values after ATCOR correction are becomes larger than an original ASTER all SWIR bands values, followed on becoming the background of vegetation from moist changes to dryness.

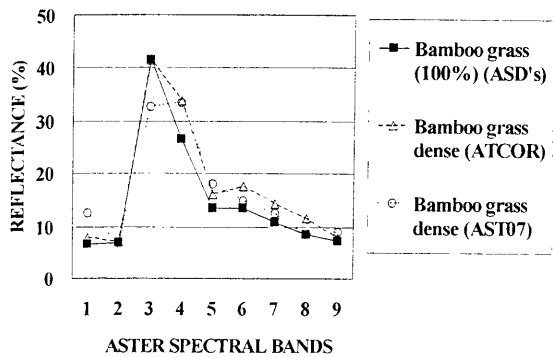


Fig. 2 (1) Comparison of the spectral reflectance of non-moor plant Bamboo grass calculated form ASD's measurement method, ATCOR method and EOSDIS AST07 method.

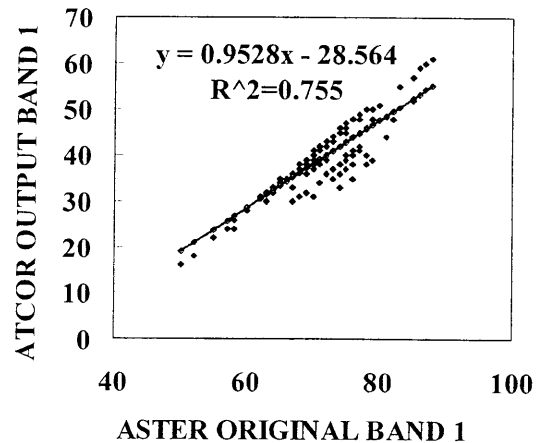


Fig. 3(1) The correlation coefficient of the ASTER original band 1 (Green) and ATCOR output band 1 (Green).

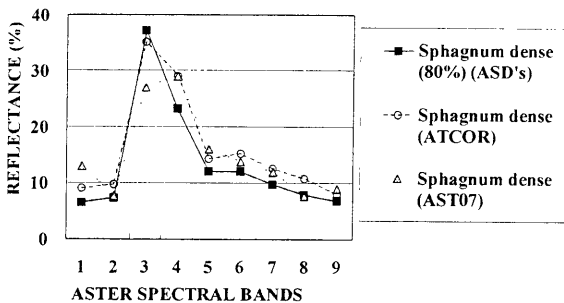


Fig. 2 (2) Comparison of the spectral reflectance of high moor plant *Sphagnum* marsh calculated form ASD's measurement method, ATCOR method and EOSDIS AST07 method.

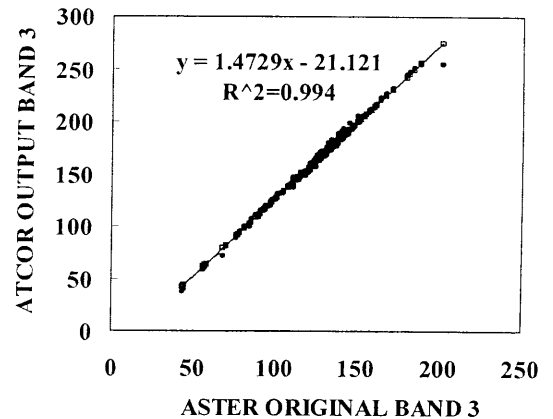


Fig. 3(2) The correlation coefficient of the ASTER original band 3 (NIR) and ATCOR output band 3 (NIR)

ATCOR have rectified more correctly scattering with short wavelength visible ((i.e. Green band) and absorption with NIR band. Shows the Fig. 3(1) and 3(2), it is clear that 5% of scattering radiation is contained with the green band and 47% of radiation was absorbed in the NIR band and 17% of radiation was absorbed in the SWIR6 band.

The input (x: DN of original ASTER L1B data) and output (y: DN of after ATCOR software atmospheric corrected ASTER L1B data) expression of the ASTER data using ATCOR are as follows:

$$\text{Green band (band 1): } y = 0.95x - 28.56 \quad (2)$$

$$\text{NIR band (band 3): } y = 1.473x - 21.12 \quad (3)$$

$$\text{SWIR band (band 6): } y = 1.171x - 1.23 \quad (4)$$

Comparison of NDVI of ground ASD's measurement, atmospheric corrected ASTER data and not atmospheric corrected original ASTER L1B data, we found that the ground NDVI and atmospheric corrected NDVI was not difference. However, the value of NDVI of ASTER L1B is smaller than the value of grand NDVI. Where, the formula of the correlation of a NDVI-Corrected value and an original ASTER L1B NDVI value is as follows:

$$NDVI_{corrected} = 1.27 \times NDVI_{L1B} + 0.04 \quad (5)$$

This formula showed that the NDVI value after atmospheric correction became larger than atmospheric correction before.

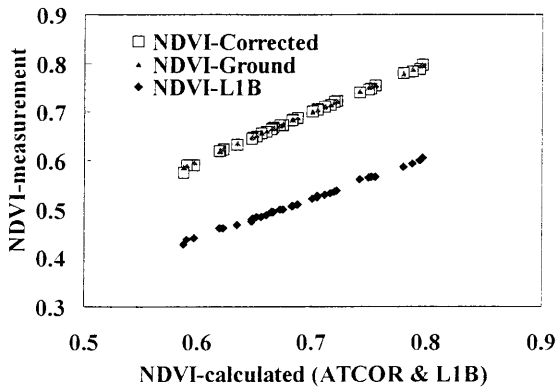


Fig. 3(3) Comparison of NDVI of ground measurement, atmospheric corrected ASTER LIB data and not atmospheric corrected original ASTER LIB data

V. CONCLUSION

Many techniques have been developed which determine the contribution atmospheric scattering has on the radiation detected by the satellite sensor. The radiance received from a target against a background surface by the satellite sensor comes from a combination of three sources; first, the intrinsic radiance reflected by the target and then directly transmitted by the atmosphere; secondly, the radiant energy scattered diffusely by the atmosphere which then further interacts with the target background and thirdly the radiant energy scattered diffusely by the atmosphere. The radiant energy reflected by the target carries the direct energy from the target. The other two sources produce a combined effect.

Atmospheric measurements and modeling involves the theoretical determination of the path radiance contribution of the atmosphere for the particular time of the overpass. To calculate the contribution of the scattering on the reflected radiance requires that many atmospheric variables at the time of the satellite overpass be recorded and inputted into theoretically derived equations to determine the effect of the atmosphere on each spectral band.

For the ASTER original LIB data (Jun 30, 2001), the statistics mean value of Green band and NIR band is 50.9 and 69.8 to after atmospheric correction, the statistics mean value of Green band and NIR band is 26.5 and 90.9. (For the ASTER/July 12, 2004 case, that the values was 53.8 and 83.5 to 27.5 and 131.4 respectively). The value of NDVI after atmospheric correction is larger than atmospheric correction before, and this rate of change is $(\text{NDVI-Corrected}) = 1.27 (\text{NDVI-LIB}) + 0.04$.

Comparison of accuracy of the ATCOR software atmosphere correction of non-moor plant and high moor plant area ASTER imagery showed that the background soil and leaf area affected the accuracy of ATCOR. In the case of a moor plant, the error in ASTER Green band is large.

Acknowledgment

This study was supported in part by the Scientific Research Project from the Department of Advancement of Science and Technology in the Hokkaido Government; and the Scientific Research Project No. {03-01-03 103-021017}. The authors' deep appreciation is expressed to Dr. Mark J. Chopping, from the Montclair State University, USA for the valuable comments on the manuscript.

REFERENCES

- [1] Schott J.R. and Henderson-Sellers, A., "Radiation, the Atmosphere and Satellite Sensors. Contribution in Satellite Sensing of a Cloudy Atmosphere: Observing the Third Planet (Ed: Henderson-Sellers)," 1984, pp45-89.
- [2] Campbell, J. B., "Introduction to Remote Sensing: Second Edition," The Guilford Press, New York, 1996, pp. 444-476.
- [3] W G Rees, " Physical Principles of Remote Sensing, Second Edition, " Cambridge University Press, 2001, pp. 76-85.
- [4] Kneizys, F.X., "Atmospheric Transmittance Radiance: computer code " LOWTRAN AFGL-TR-83-0187 (1983).
- [5] Berk, A., L. S. Bernstein, and D. C. Robertson, "MODTRAN. A Moderate Resolution Model for LOWTRAN 7," GL-TR-89-0122, Phillips Laboratory, Geophysics Directorate, Hanscom Air Force Base, Massachusetts, 1989.
- [6] Berk, A., L.S. Bernstein, G.P. Anderson, P.K. Acharya, D.C. Robertson, J.H., "Chetwynd and S.M. Adler-Golden, MODTRAN Cloud and Multiple Scattering Upgrades with Application to AVIRIS.," Remote Sens. Environ, 1998, pp.65:367-375.
- [7] E. Vermote, D. Tanr, J. Deuz, M. Herman, and J. Morcette, "Second simulation of the satellite signal in the solar spectrum 6S: An overview," IEEE Trans. Geosci. Remote Sensing, vol. 35, no. 3, 1997, pp. 675-686.
- [8] Fraser, R. S, R. A. Ferrare, Y. J. Kaufman, B. L. Markham, S. Mattoo, "Algorithm for atmospheric correction of aircraft and satellite imagery," Int'l. J. Rem. Sens., 1992, pp.13:541-557.
- [9] R. Richter, "A fast atmospheric correction algorithm applied to Landsat TM," Int. J. Remote Sensing 1990, pp.11:159-166.
- [10] Crippen, R.E., "The Regression Intersection Method of Adjusting Image Data for Band Ratioing," *International Journal of Remote Sensing*, Vol. 8, No. 2, 1987, pp. 137-155.
- [11] Chavez, P. S., Jr., "An improved dark-object subtraction technique for atmospheric scattering correction of multispectral data," *Remote Sens. Environ.*, 24, 1988, pp. 459-479.
- [12] Liang, S., H. Fang, J. Morissette, M. Chen, C. Walthall, C. Daughtry, and C. Shuey, "Atmospheric Correction of Landsat ETM+ Land Surface Imagery: II. Validation and Applications," *IEEE Transactions on Geosciences and Remote Sensing*, 40(12): 2002, pp.2736-2746.
- [13] Buhe Aosier, K. Tsuchiya, M. Kaneko, S. J. Saiha, "Comparison of Image Data Acquired with AVHRR, MODIS, ETM+, and ASTER Over Hokkaido Japan," *Advances in Space Research*, Vol. 32, No. 11, 2003, pp.2211-2216.
- [14] Herman, B. M., & Browning, S. R., "A numerical solution to the equation of radiative transfer," *Journal of the Atmospheric Sciences*, 22, 1965, pp.559-566.
- [15] Slater, P. N., Biggar, S. F., Holm, R. G., Jackson, R. D., Mao, Y., Moran, M. M., Palmer, J. M., & Yuan, B., "Reflectance- and radiance-based methods for the in-flight absolute calibration of multispectral sensors," *Remote Sensing of Environment*, 1987, pp.22, 11 - 37.

- [16] Drury, S.A., "Image Interpretation in Geology. Allen and Unwin (Publishers) Ltd, London. Forster, B.C. (1980). Urban residential ground cover using Landsat digital data. Photogram, " Eng. Remote. Sen. 46, 547, 1987, pp.58.
- [17] Coops, N.C., Culvenor, "Utilizing local variance of simulated high-spatial resolution imagery to predict spatial pattern of forest stands, " Remote Sensing of Environment. 71(3): 2000, pp.248-260.